CHAPTER X

Sorption and Desorption of diquat^{2+} on Na-Molecular Sieve - 13X System.

Molecular sieves are found to be most versatile, selective and universally applicable adsorbents available to industry. So the study of the use of molecular sieve in adsorption and catalysis is of great significance in industry and has deservedly received a great deal of interest in recent years. Zeolites as synthesized or formed in nature, are crystalline, hydrated alumino silicates of group I and II elements. Structurally they comprise a framework based on an infinitely extending three-dimensional network of SiO_4 and AlO_4 tetrahedra linked together through common oxygen atoms. The isomorphic substitution of silicon by aluminium gives rise to a net negative charge compensated by cations. Zeolites can be represented by the empirical formula,

$$M_{2/n}O.\ Al_2O_3.\ x\,SiO_2.\ y\,H_2O,$$

where M is the compensating cation with valency n. In this oxide formula x is generally equal to or greater than 2 (212) since AlO_4 tetrahedra are joined only to SiO_4 tetrahedra. The structural formula of a zeolite can be represented by its unit cell composition:

$$M_{x/n}[(AlO_2)_x(SiO_2)_y] \cdot ZH_2O \cdot$$

The ratio y/x usually has a value of 1-5 depending upon the structure. The framework structures of zeolites are composed of arrangements of tetrahedra in building units going from ring structures to polyhedra. Usually, zeolites are classified using common structural units. Zeolites A, X and Y consist of linked cubooctahedra (β cages or 24-hedra). Such a polyhedron, also called a sodalite unit, has a central cage of diameter 0.65 nm, accessible through six membered rings of oxygen atoms with a free diameter of 0.22 nm. In the mineral faujasite and the synthetic faujasites (zeolites X and Y), the cubooctahedra are linked with bridging oxygen atoms but in a tetrahedral symmetry. The sodalite units connected along two six-membered rings give rise to hexagonal prism. In this way, the polyhedra enclose a supercage with an internal diameter of 1.25 nm and accessible through four twelve-membered rings of oxygen atoms with a free aperture of 0.75 nm.

Owing to the isomorphic substitution of Si by Al, the three dimensional oxygen framework carries an excess negative charge, compensated by cations. These cations can be exchanged by other cations of different nature

and valency. Not only simple cations can be exchanged but also complexes of cations such as $Cu(NH_3)_4^{2+}$ and $Pt(NH_3)_4^{2+}$. The only limitation to the nature of the cations that can be introduced by ion exchange is the acid stability of the zeolite. Generally, zeolites with higher Si : Al ratio are more acid stable. Sieving of one type of molecule out of a feed containing a mixture of molecules with different shapes and/or sizes, is possible because the free apertures of the zeolites have molecular dimensions.

The ion exchange behaviour of some transition metal ions in zeolite A was studied by Gal et al (278), and in zeolite X by Wolff et al (279, 280) and Maes et al (225). Although several studies on molecular sieve X and Y involving inorganic and organic ions (214, 215, 221, 222, 223) have been reported in literature, such study with the herbicide, diquat, is still lacking. So, in this section, are presented the sorption characteristics of diquat^{2+} on Linde Molecular Sieve-13X (powder form supplied by B.D.H. Chemicals Ltd., England, as gift) and its desorption from the adsorbent complex by monovalent and bivalent inorganic and organic ions in line with similar studies reported earlier with clay and resin systems.

Before use, the molecular sieve-13X was saturated with 1M NaCl solution and dialysed against distilled water

until free of chloride (225). They were then dried at 50°C, ground and stored at room temperature over saturated NH_4Cl solution in a desiccator for at least a week. Then it was used for the exchange of diquat^{2+}. The Na-molecular sieve X-diquat complex was used for desorption studies. The experimental procedures for studying the exchange of diquat^{2+} was almost similar to the clay minerals and resins. About 0.1 gm of NaX was weighed into pyrex bottles to which increasing amounts of standard diquat aqueous solution were added. The total volume was kept constant (15 ml) in each case by adding the requisite amount of water. They were then shaken for four hours and kept overnight to attain equilibrium. The aliquots were then centrifuged for about 20 minutes and the amount exchanged was determined from absorbance of the supernatants using a DU-2 spectrophotometer.

Similarly, for desorption study the dry Na-sieve X-diquat complex was weighed accurately ($\simeq$ 0.1 gm) in different pyrex bottles to which varying amounts of desorbing electrolytes were added. The volume was kept constant (15 ml) in each case by adding the necessary amount of deionised water. They were also shaken for 4 hours and kept overnight (48 hrs for organic electrolytes) and diquat content of the supernatants was measured as above.

SECTION A

Sorption Studies

Sorption of diquat on Na-Molecular Sieve 13X.

The exchange isotherm of diquat^{2+} on Na-Sieve-X is shown in Fig. 85, which is of the Langmuir type indicating strong interaction between the herbicide cation and the adsorbent. The plot of C/x against C (Fig. 85) is, accordingly, linear. From the slope of the line, the value of V_m is found to be 117.64 me/100 gm which corresponds to the maximum exchange from the isotherm (116 me/100 gm).

The value of V_m is, however, found to be much less than the total exchange capacity of the sieve-13X i.e. 632 me/100 gm (281). Thus the isotherm shows maximum exchange of about 18.35% for diquat^{2+}. Steric factors based on cation size relative to the zeolite aperture diameters may explain the partial ion-sieve effect and incomplete exchange observed with diquat^{2+} ion in zeolite-X. The observations of Vansant and Vanhoof (224) may be recalled here where for steric reasons, organic cations (alkanediammonium ions) could not effect a complete replacement of Na^+ initially present in the zeolites, so that the exchange reactions were confined to the large cavities in the crystal.

Differential Thermal Analysis studies on Na-mol-sieve-13X-diquat complex :

The Na-molecular sieve-13X fully exchanged with diquat^{2+} prepared as described earlier, was stored over concentrated sulphuric acid for 20 hours prior to analysis. The result is shown in Fig. 86. The results of thermogravimetric analysis clearly distinguish the various thermal reactions occurring over different ranges of temperature. The strong endothermic peak at 190^{o}C in the DTA curve may be related to the loss of water of the zeolite-diquat complex. The exothermic peak at about $\simeq$ 270^{o}C probably signifies the desorption of the exchanged adsorbate from the solid matrix. This is followed by a high temperature dehydration endothermic peak at 290^{o}C. The exothermic peak at 375^{o}C and a sharp peak at 455^{o}C possibly correspond to the oxidation and decomposition of the diquat. The weaker exothermic peak at 892^{o}C probably accompanies the destruction of the hydrated zeolite and the formation of sintered amorphous phase of β-carnegite (261).

From the TG curve (Fig. 86), the loss of weight of the Na-molecular sieve-13X-diquat complex is recorded in Table - 15.

Table - 15

Temperatures in °C	50°C	100°C	200°C	400°C	500°C	800°C	900°C
Weight loss in mg per 100 mg of Na-mol.-Sieve-13X-diquat.	1.7	4	14	23	28	28.5	28.8

The great loss in weight at 200°C corresponds to the loss of zeolitic water of the adsorbent while the greater loss in weight at 500°C corresponds to the decomposition and pyrolysis of the organic herbicide after which it remains almost constant upto 940°C. The DTG downward peaks (Fig. 86) at 200°C, 460°C also support the above facts.

SECTION B

Studies on Desorption

Desorption of diquat^{2+} from Na-mol-Sieve-13X-diquat

The results of desorption of diquat^{2+} from its Na-Sieve-13X-diquat complex are shown in Figs. 87, 88, 89, 90, 91, 92. According to the Fig. 87 and the selectivity coefficients (Table - 16), the monovalent ions may be placed at low concentrations in the order: $Li^+ < Na^+ < Cs^+ < Rb^+ < NH_4^+ < K^+$ while at higher concentrations the sequence is $Li^+ < Cs^+ < Rb^+ < Na^+ < NH_4^+ < K^+$. For bivalent Cations (Fig. 88), both at low and high concentrations, the order of desorption is $Mg^{2+} << Ca^{2+} << Sr^{2+} < Ba^{2+}$. The difference in selectivities for bivalent inorganic cations with increasing ionic size is more pronounced in this case which has not been observed in cases of clays and resins. Barrer et al (221) observed that for a low degree of cross-linking of polystyrene sulphonate resin selectivity was in the order: $Na^+ > Cs^+ > K^+ > Li^+ > H^+$, while with a high degree of cross linking, with limited swelling, the selectivity sequence was changed to $Na^+ > Li^+ > H^+ > Cs^+ > K^+$. Molecular sieve-X is to be regarded as an extremely highly cross linked condensation polymer, virtually non-swelling, but neither of the above sequences correlates with that observed in the case of the molecular sieve.

Both the hydrated ionic radius and the reciprocal of the Debye-Huckel parameter, a^0, for the bivalent

Table - 16

Desorption characteristics of diquat^{2+} with respect to different ions from Na-molecular-Sieve-13X-diquat.

Electrolyte used	Concentration of the electrolyte (M)	Distribution Coefficient	Selectivity Coefficient
1:1 Electrolyte			
	0.05	0.35	0.0029
LiCl	0.1	0.40	0.0052
	0.3	0.48	0.0124
	0.5	0.49	0.0172
	0.75	0.67	0.0294
	0.05	2.33	0.0530
NaCl	0.1	2.15	0.0701
	0.3	1.30	0.0629
	0.5	0.98	0.0579
	0.75	0.77	0.0528
	0.05	12.41	0.3817
KCl	0.1	6.35	0.4701
	0.3	2.17	0.1675
	0.5	1.34	0.1082
	0.75	0.91	0.0751

Contd..

Table - 16 (Contd..)

Electrolyte used	Concentration of the electrolyte (M)	Distribution Coefficient	Selectivity Coefficient
	0.05	10.70	0.6606
NH_4Cl	0.10	5.82	0.3933
	0.30	2.09	0.1551
	0.50	1.28	0.0973
	0.75	0.86	0.0668
	0.02	21.30	1.0672
RbCl	0.05	11.55	0.7653
	0.1	6.11	0.4346
	0.3	2.05	0.1492
	0.5	1.23	0.0893
	0.02	11.92	0.4068
CsCl	0.05	8.63	0.4470
	0.1	5.46	0.3476
	0.3	1.98	0.1379
	0.5	1.19	0.0832

Contd..

Table - 16 (Contd..)

Electrolyte used	Concentration of the electrolyte (M)	Distribution Coefficient	Selectivity Coefficient
2:1 Electrolytes			
	0.02	2.16	0.0301
$MgCl_2$	0.05	1.61	0.0268
	0.1	1.18	0.0207
	0.2	0.87	0.0160
	0.3	0.75	0.0144
	0.02	3.42	0.0780
$CaCl_2$	0.05	2.46	0.0650
	0.1	1.92	0.0574
	0.2	1.53	0.0532
	0.3	1.33	0.0498
	0.02	5.20	0.1918
$SrCl_2$	0.05	3.61	0.1526
	0.1	2.74	0.1296
	0.2	2.03	0.1025
	0.3	1.67	0.0855

Contd..

Table - 16 (Contd..)

Electrolyte used	Concentration of the electrolyte (M)	Distribution Coefficient	Selectivity Coefficient
	0.02	6.12	0.2802
$BaCl_2$	0.05	4.01	0.1964
	0.1	2.88	0.1468
	0.2	2.07	0.1086
	0.3	1.70	0.0896
Quaternary ammonium salts			
	0.1	0.004	$0.06 \times 10^{-}$
	0.2	0.007	0.18 "
$(CH_3)_4NBr$	0.3	0.012	0.60 "
	0.4	0.017	0.92 "
	0.5	0.022	1.49 "
	0.1	0.025	0.82 "
$(C_2H_5)_4NBr$	0.2	0.022	0.93 "
	0.3	0.017	0.82 "
	0.4	0.014	0.70 "
	0.5	0.011	0.56 "

Contd..

Table - 16 (Contd..)

Electrolyte used	Concentration of the electrolyte (M)	Distribution Coefficient	Selectivity Coefficient
	0.1	0.014	0.33×10^{-4}
$(C_3H_7)_4NBr$	0.2	0.011	0.35 x "
	0.3	0.010	0.35 x "
	0.4	0.008	0.33 x "
	0.5	0.007	0.31 x "
	0.1	0.011	0.25 x "
$(C_4H_9)_4NBr$	0.2	0.010	0.30 x "
	0.3	0.007	0.24 x "
	0.4	0.007	0.23 x "
	0.5	0.006	0.20 x "
DTABr	0.002	1.22	0.0038
	0.004	0.78	0.0027
	0.006	0.54	0.0019
	0.008	0.42	0.0015
	0.010	0.34	0.0013

Contd..

Table - 16 (Contd..)

Electrolyte used	Concentration of the electrolyte (M)	Distribution Coefficient	Selectivity Coefficient
	0.002	1.63	0.0058
DDTABr	0.004	1.10	0.0046
	0.006	0.87	0.0040
	0.008	0.72	0.0035
	0.010	0.62	0.0031
	0.002	2.39	0.0104
CTABr	0.004	1.39	0.0066
	0.006	0.98	0.0048
	0.008	0.78	0.0039
	0.010	0.65	0.0033
	0.002	2.97	0.0145
CPCl	0.004	1.80	0.0170
	0.006	1.35	0.0077
	0.008	1.09	0.0064
	0.010	0.91	0.0055

Contd..

Table - 16 (Contd..)

Electrolyte used	Concentration of the electrolyte (M)	Distribution Coefficient	Selectivity Coefficient
Alkane diammonium salt			
	0.002	8.70	0.1500
EDA	0.005	8.05	0.2125
	0.01	7.25	0.2586
	0.03	4.82	0.2122
	0.05	3.78	0.1709
	0.002	7.00	0.0976
PrDA	0.005	7.00	0.1594
	0.01	6.81	0.2253
	0.03	4.62	0.1920
	0.05	3.67	0.1590
	0.002	5.65	0.0638
BuDA	0.005	4.88	0.0765
	0.01	4.06	0.0762
	0.03	2.54	0.0522
	0.05	1.97	0.0405

inorganic ions when plotted against logarithm of selectivity coefficient (Fig. 92) give linear graphs while for the monovalent inorganic ions, only the latter plot is linear as observed earlier in clays and resins.

The exchange isotherms with tetraalkylammonium ions are presented in Fig. 89. The percentages of the herbicide released by these ions are much smaller than the inorganic ions and the exchange is inversely related to the size of the ions. The isotherm with $(CH_3)_4N^+$ is found to be S-shaped as observed earlier in Amberlite IR-120 and Amberlite IRC-50, indicating cooperative sorption i.e. more and more exchange sites are accessible with the progress of exchange. Because of its rigid three-dimensional framework enclosing cavities, which are entered through windows of definite dimensions, exchange in molecular sieve 13X is greatly influenced by steric and space factors. Thus, using concentrated solutions of various methyl and ethylammonium halides, Barrer et al (221) reported virtually complete exclusion of the tetraethylammonium ion whilst the methylammonium derivatives gave upper limits to exchange which decreased as the number of alkyl groups in the cation increased. Ion sieve action of this type is encountered in all members of the zeolite groups of minerals (272). With the long-chain

surface active ions (Fig. 90), however, the extent of exchange increases with the chain length of the ions, although the maximum desorption with CP^+ did not exceed even one percent.

Compared to other organic ions, the upper limits of exchange with the alkanediammonium ions are much higher (Fig. 91), although an inverse relation was observed between the maximum exchange and the molecular weight as noticed earlier in Amberlite IR-120 (P-161). A similar observation has been made by Vansant and Vanhoof (224) and has been attributed to the space requirement of the ions and difficulty of packing of the organic ions in the rigid non swelling zeolite matrix. Due to their short-chain structure, possibly these ions experience less steric hindrance and also owing to their double charge sites in the structure, probably, an important contribution of van der Waals interaction causes the greater affinity of the alkanediammonium ions for the molecular sieve-13X.

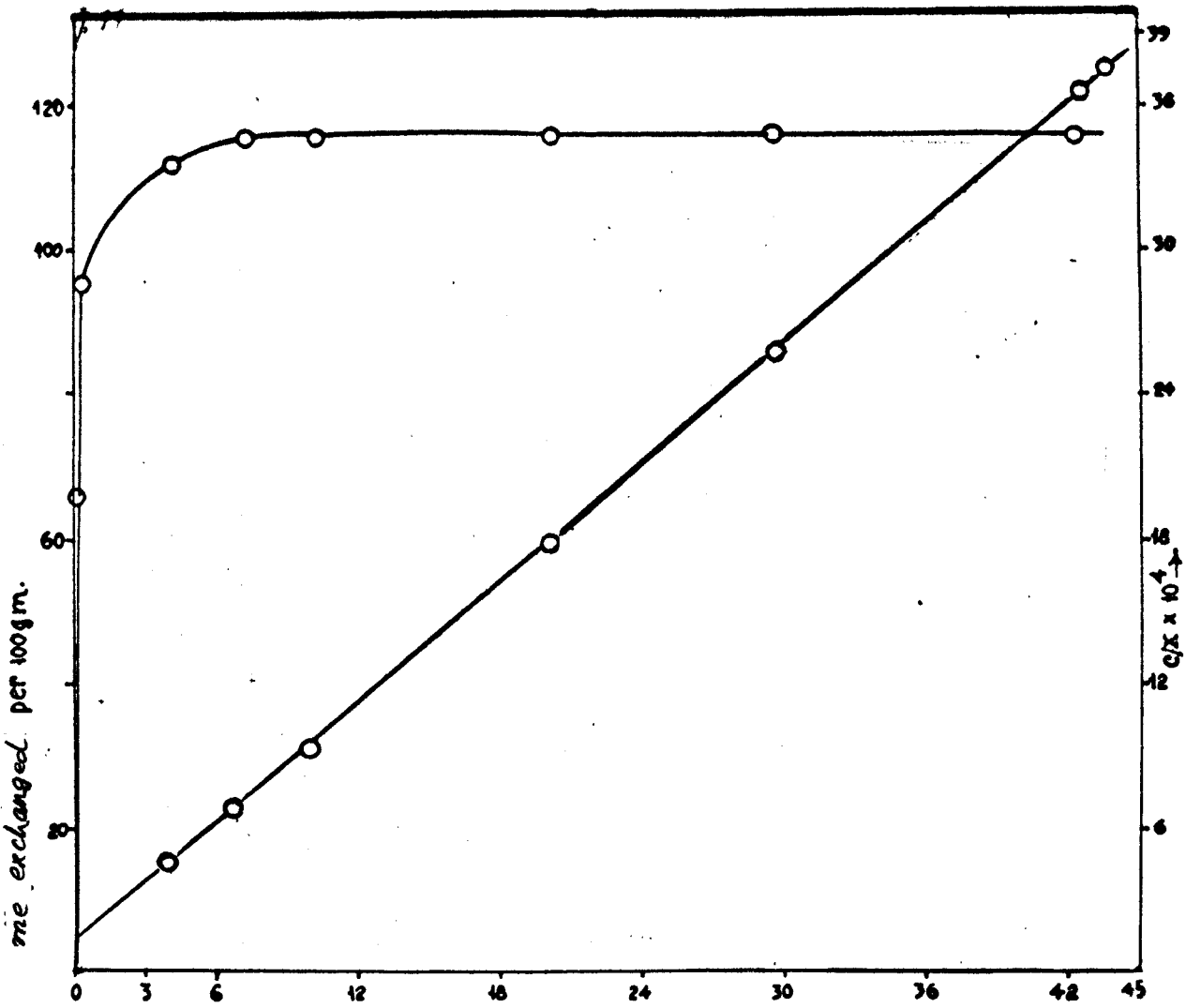

Fig. 85. Exchange isotherm of diquat on molecular sieve-13X.

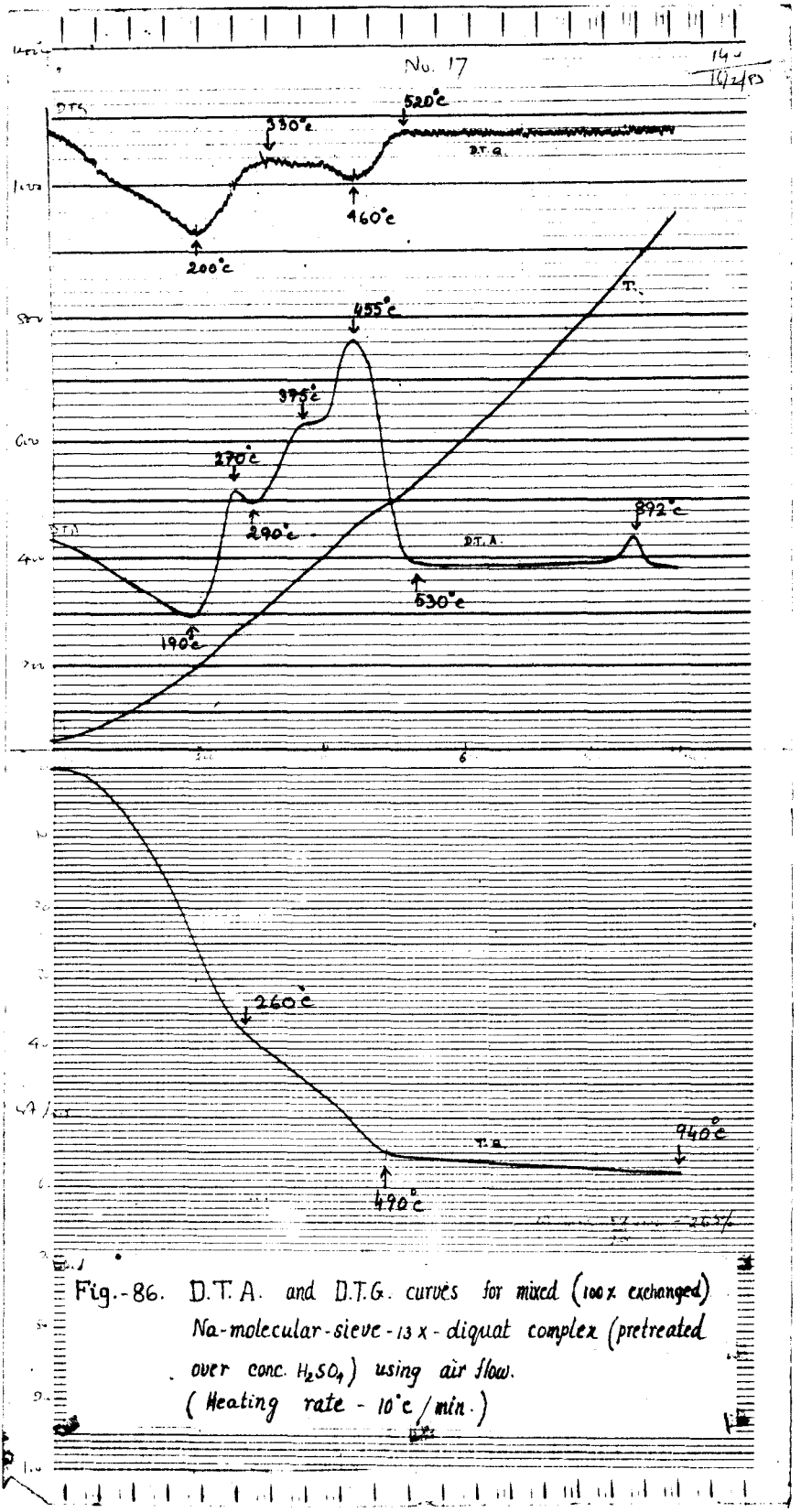

Fig.-86. D.T.A. and D.T.G. curves for mixed (100% exchanged) Na-molecular-sieve-13x-diquat complex (pretreated over conc. H_2SO_4) using air flow. (Heating rate - 10°c/min.)

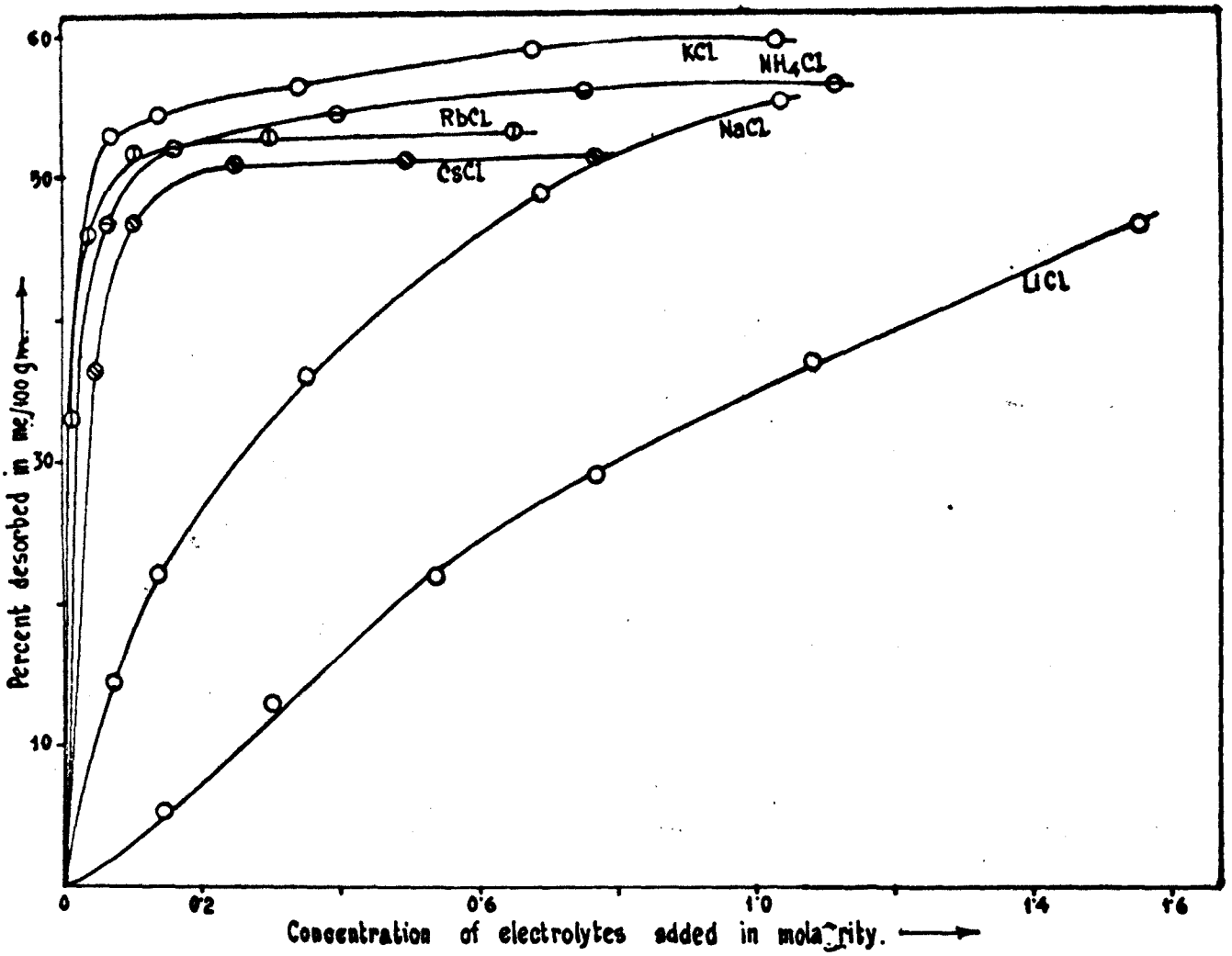

Fig. 87. . Desorption isotherms of diquat from Na-mol.-sieve-diquat by monovalent inorganic ions.

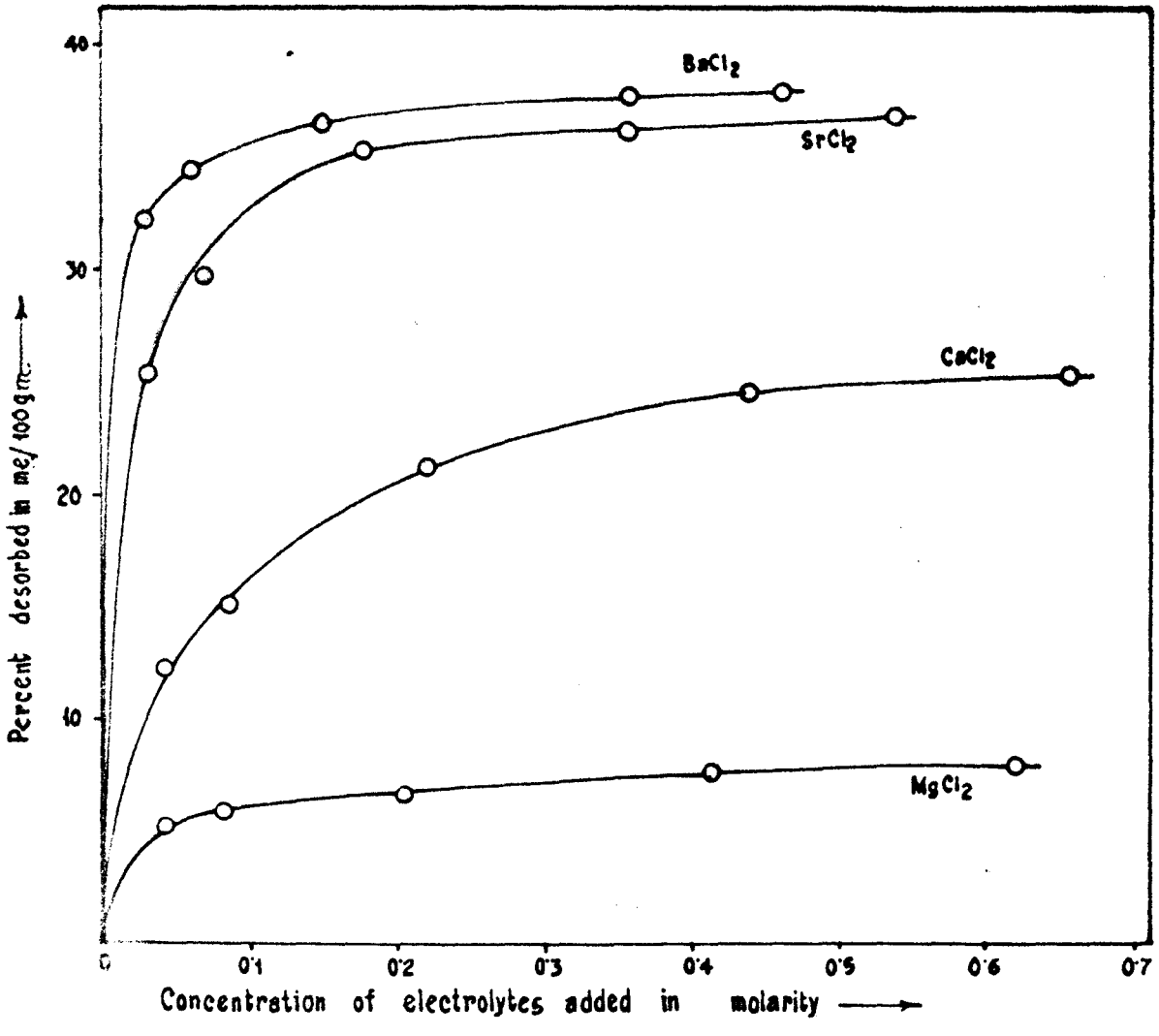

Fig. 88. Desorption isotherms of diquat from Na-mol-sieve-diquat by bivalent inorganic ions.

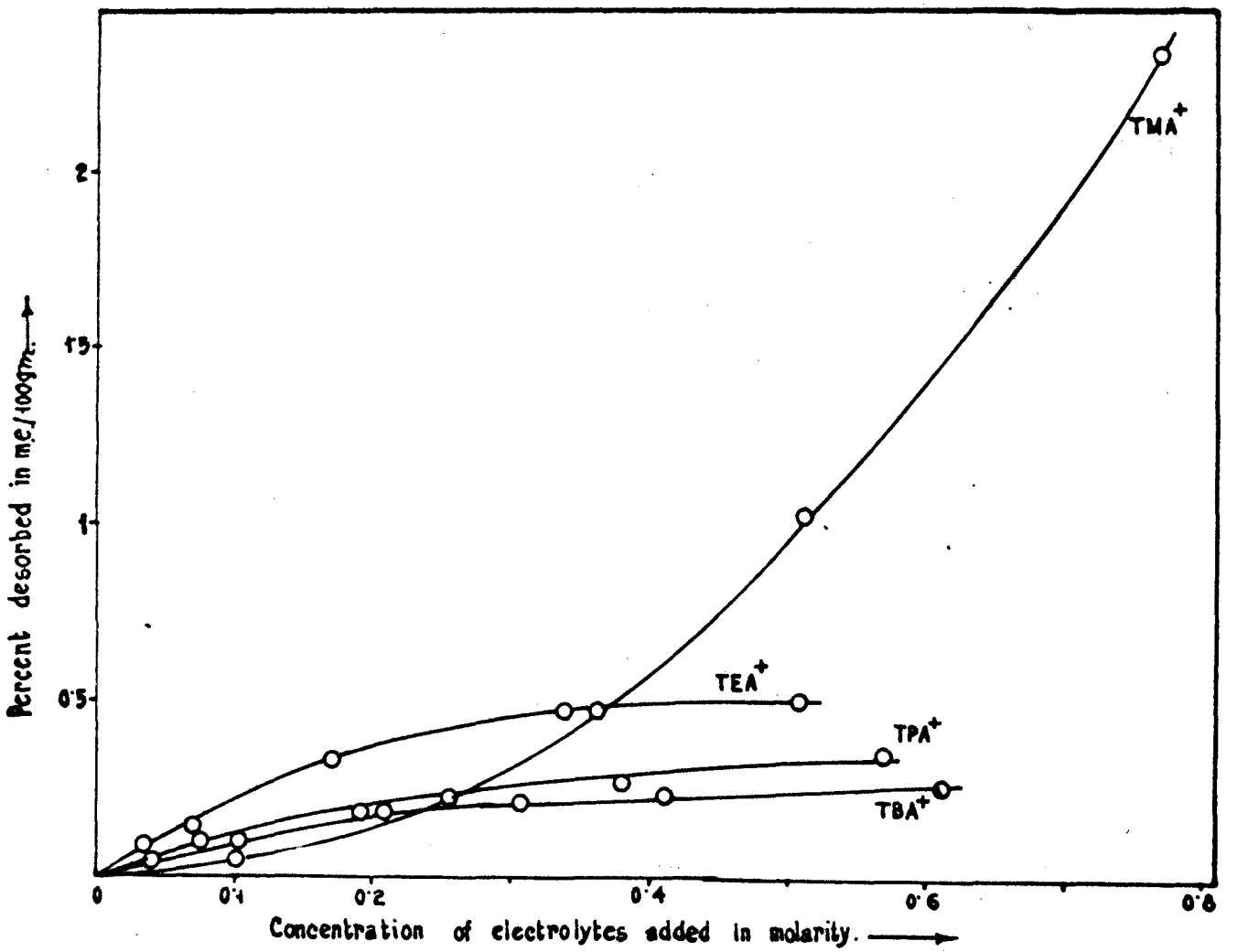

Fig. 89. · Desorption isotherms of diquat from Na-mol.-sieve-diquat by monovalent organic ions.

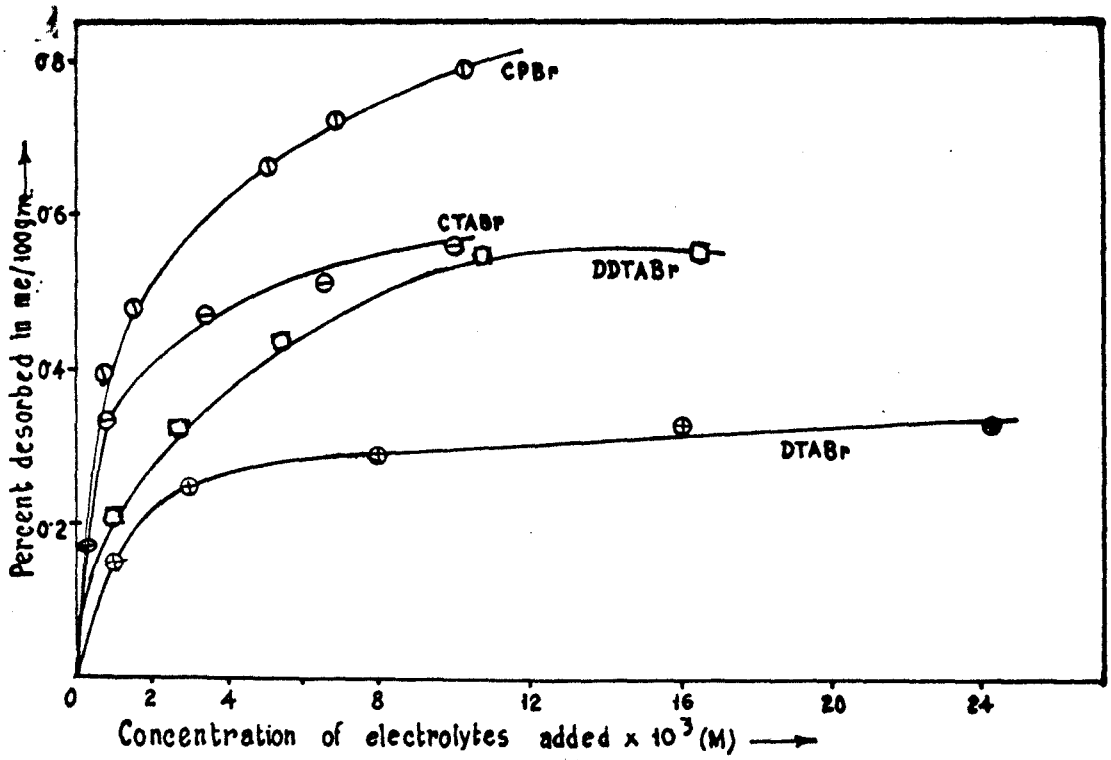

Fig. 90. Desorption isotherms of diquat from Na-mol.sieve-diquat by monovalent organic ions.

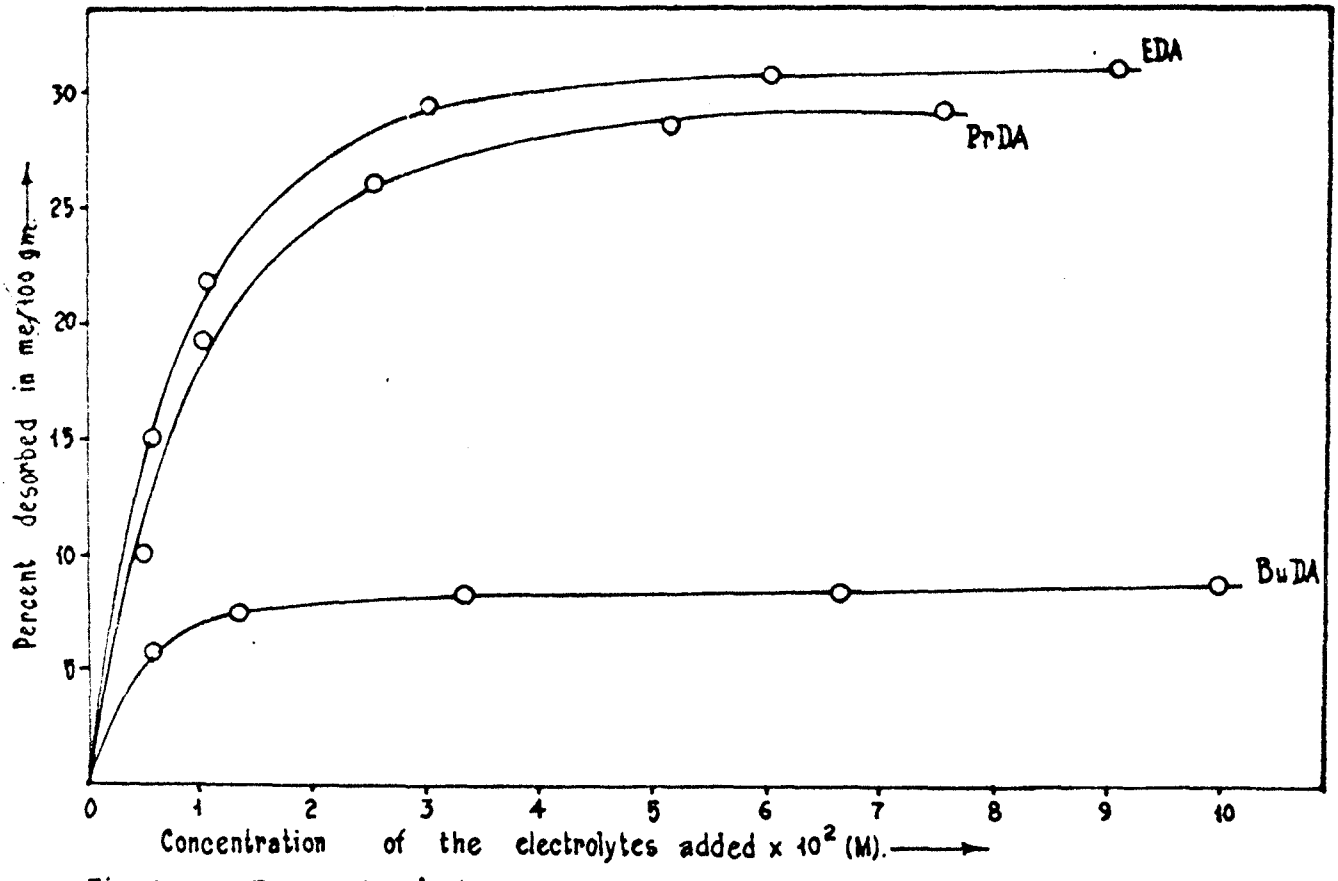

Fig. 91. Desorption isotherm s of diquat from Na-mol-sieve-diquat by bivalent organic ions.

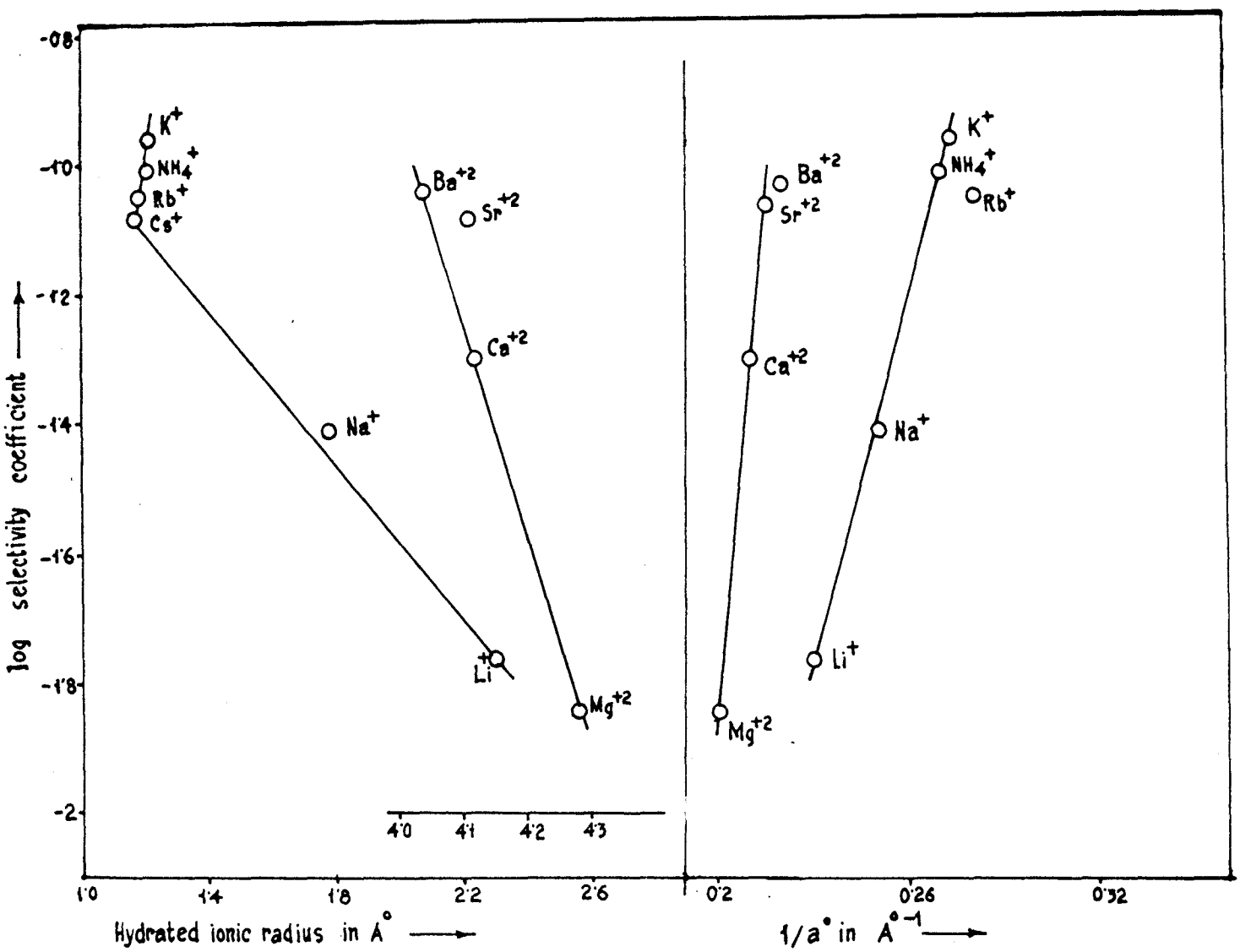

Fig. 92. Correlation of selectivity coefficient with hydrated ionic radius and Debye-Hückel parameter a° in the desorption of diquat from Na-molecular sieve-13x-diquat.

CHAPTER XI

Summary and Conclusion

The structures of the clay minerals, namely, kaolinite, montmorillonite, vermiculite, Laponite are briefly discussed. A short review of the earlier work on adsorption and desorption of inorganic and organic ions and the herbicide diquat^{2+} on clay minerals and other model adsorbents such as resins and molecular sieves is presented in the introductory Chapter I (PP 1-52).

The methods of analyses and the preparation of materials, experimental details and the preparation of samples for I.R. spectra, X-ray diffraction, DTA/DTG analysis are described in Chapter III (PP. 58-65).

The adsorption isotherm of diquat^{2+} on H-bentonite and Na-bentonite are of the H-type, indicative of strong sorbate-sorbent interactions and of species adsorbed flat on the surface. The adsorption data of diquat^{2+} on H-bentonite and Na-bentonite are found to fit in with the Langmuir equation. The amount of diquat^{2+} adsorbed on H-bentonite is less than the c.e.c. of the clay. This may be due to the low pH of the solution but as the pH is increased, the adsorption of diquat^{2+} increases, indicating that two categories of H^{+} are present in bentonite.

Adsorption at low pH probably corresponds to exchange due to isomorphous lattice replacement whereas

the higher adsorption at higher pH corresponds to the sorption at the edges primarily caused by Si-O and Al-O sites. X-ray diffraction, i.r. spectra and DTA/DTG studies of Na-bentonite-diquat complex throw considerable light on the mechanism of interaction. X-ray diffraction examination of the bentonite-diquat complex suggests that the herbicide cation is evidently intercalated by bentonite and the plane of the rings lies parallel to the silicate layers, thus affording close van der Waals contact between the molecule and the clay surface. Ultraviolet and infrared spectroscopic measurements of the bentonite-diquat complex indicate that charge-transfer between the organic cation and the bentonite acting as an electron donating anion because of lattice substitution, may be involved even at low degrees of saturation of the herbicide in the clay, reinforcing the normal coulombic attractive forces. So it appears that although cation exchange is the principal mechanism of adsorption of diquat^{2+}on bentonite, van der Waals and charge-transfer processes may also contribute to the strong electrostatic attraction between the herbicide and the clay. The DTA/DTG curves of bentonite-diquat complex show that the clay complex is very stable upto higher temperatures.

The efficiency of the inorganic ions in desorbing diquat^{2+} from the Na-bentonite matrix generally increases

with the crystallographic radius of the ions. The orders of selectivity for the monovalent and bivalent ions are: Cs > Rb > K > NH_4 > H > Na > Li and Ba > Sr > Ca > Mg . The variable position of the H^+ in the series is well known for which the idea of bare proton taking part in exchange reaction has been invoked. The plots of log (sselectivity coefficient) against hydrated ionic radius and the reciprocal of the Debye Huckel parameter, a^o, yield straight lines in the case of alkaline earth metal cations while for the alkali metal ions the latter plot is only linear. The cause of non linearity in the case of alkali metal ions has been attributed to the unequal fixation tendencies of the ions vis-va-vis interlayer collapse of the clay structure (P 87). However, the plot of log (selectivity coefficient) vs $1/a^o$ is on the basis of simple ion-exchange model of Pauley, which suggests that electrostatic attraction between the counterions and the fixed ionic groups is the significant factor. The above plots clearly demonstrate that in the exchange of bivalent diquat^{2+}ion from the clay matrix by alkali metal ions, only $1/a^o$ may be used to correlate and predict the relative affinities of the ions for the mineral while for the alkaline earth metal ions, both hydrated ionic radius and $1/a^o$ may be used for the purpose.

Interestingly, the exchanging ability of the tetraalkylammonium ions is found to be inversely related to the size of the ions, which is in sharp contrast with general behaviour of the adsorption of organic compounds in bentonite. This behaviour has been explained by assuming contraction of silicate layers due to the strong electrostatic attraction between the herbicide cation and the clay. The coulombic forces of the resulting bentonite-diquat complex are too strong for layer expansion required for easy entry of the large tetraalkylammonium ions into the interlameller region for the exchange to occur and hence the extent of exchange decreases with the size of the ions. This has been justified from the measurement of d_{001} spacings of Na-bentonite-diquat, Na-bentonite-diquat-$(CH_3)_4^{*}N$ and Na-bentonite-diquat-$(C_4H_9)_4^{*}N$ systems which are 13.32, 13.67, 13.39 A^{o} respectively at 51% r.h., suggesting little penetration of the large tetraalkylammonium ions into the interlameller space. The observed exchange order $(CH_3)_4N^{+} > (C_2H_5)_4N^{+} > (C_3H_7)_4N^{+} > (C_4H_9)_4N^{+}$ in bentonite has been rationalized in terms of the hydration energies and van der Waals forces of these ions vis-a-vis the energy requirement for layer expansion for entry of these large ions (P 84). The desorbing efficiency

---

* Corresponding to maximum of the desorption isotherm.

of the long-chain surface active ions and alkanediammonium ions, however, increases with chain length of the ions and may be attributed to the increased contribution of van der Waals forces to adsorption energy as well as to change in the hydration status of the ions in the clay interlayer. This behaviour would, however, be expected for a flat orientation of the ions onto the surface as van der Waals forces are additive and increase with increasing chain length. The exchangeability of CP^+ or CTA^+ is much higher than the tetraalkylammonium and alkanediammonium ions. This is probably due to the fact that in CP^+ or CTA^+, the van der Waals force is large because of long aliphatic carbon chain and hence expansion of silicate layers is permitted, at least partially. As a result, the exchange of $diquat^{2+}$ by CP^+ or CTA^+ is greater than by tetraalkylammonium or alkanediammonium ions. It is also interesting to note that the values of the selectivity coefficients of the former ions are much higher than the latter. This would suggest that for large organic ions size is more important than charge in determining their preference for the mineral surface as the dispersion forces increase significantly with chain length. In addition to this, the solubility of the organic cations in water decreases as the size increases and there is therefore less tendency for the larger ions, once adsorbed,

to escape back into the solution.

Although the desorption isotherms of diquat^{2+} in Na-bentonite-diquat complex are similar to those in the H-bentonite-diquat complex, the selectivity coefficients of the desorbing ions are found to be little higher in Na-bentonite system, indicating that the herbicide cation is more strongly bound in H-bentonite.

The adsorption isotherm of diquat^{2+} on Na-vermiculite is also of the H-type and the sorption data conform quite well with the linear form of the Langmuir equation. The X-ray data suggest that although interlayer penetration of the herbicide cation occurs with vermiculite, the extent of intercalation is limited since complete exchange for the Na^{+} ions initially present is not attained.

The desorption isotherms of diquat^{2+} with inorganic and organic ions are almost alike with the bentonite systems. But the percentages of desorption by inorganic as well as organic ions are higher in vermiculite compared to bentonite suggesting that the herbicide is more strongly attached to the latter mineral. Differences in charge density and hence in intercharge separation on interlayer surfaces, together with variations in stability of cation-water assemblages in the interlayer space, are invoked to

account for these observations.

As noted in bentonite, here also a sharp break is observed in the plot of log (selectivity coefficient) vs hydrated ionic radius of the alkali metal ions but when the former is plotted against $1/a^{o}$, linearity is attained. Similar plots with both the parameters with the alkaline earth metal ions yield good straight lines.

The influence of the size of big organic ions in desorption assumes importance here because in vermioulite the interlamellar space is limited to the thickness of about two water layers (4.98 $\mathring{A}$). As observed in the case of bentonite, here also the desorption of diquat^{2} is found to be inversely related to the molecular weight of the tetraalkylammonium ions. It is very probable that in this cation exchange process larger $(C_4H_9)_4N^+$ or $(C_3H_7)_4N^+$ ions experience more steric hindrance than the comparatively small $(CH_3)_4N^+$ or $(C_2H_5)_4N^+$ and the exchange takes place mostly from the edges and exterior surfaces of the mineral. This conclusion has also been confirmed from the measurement of d_{001} basal spacings (P 105) of the complexes. The extent of desorption with the bivalent alkanediammonium ions and long chain surface active ions, however, increases with chain length and CP^+ or CTA^+ desorbs larger amount of diquat^{2+} than the former ions. Similar findings were also

noted in bentonite system. The exchange data with the organic ions have been explained in terms of the size, shape, charge and hydration energies of these ions, van der Waals forces and the energy required for the expansion of the silicate layers as mentioned earlier in the case of bentonite (PP 83-86). This observation supports the argument that the interlayer spacing of the clay in suspension is of crucial importance in explaining cation preference in exchange. This is especially true of contracted, higher layer charge clays, as in vermiculite, where energy must be provided for interlayer expansion so that exchange by large cations can occur.

The sorption isotherm of diquat^{2+} on Na-Laponite XLG, a synthetic hectorite, also belongs to the H- class of isotherms and the exchange data obey the Langmuir equation. However, compared to Na-bentonite, the maximum exchange of diquat^{2+} onto Laponite, is much less than its c.e.c. This is possibly due to the fact that owing to its lower charge density than bentonite, the exchange sites in Laponite are more widely spaced and the diquat^{2+} ion with its shorter separation of charge centres (3.5 Å) could not effectively counter the adsorbent charge. The i.r. spectra of the Laponite-diquat complex also suggest

the formation of a charge-transfer complex between the herbicide cation and the anionic silicate framework as observed in bentonite.

The extent of desorption of diquat^{2+} by monovalent and bivalent inorganic ions and by the short chain alkanediammonium ions is found to be much lower than that observed in bentonite and vermiculite. As mentioned earlier, the exchange sites in Laponite are more widely spaced than the latter minerals and so the smaller inorganic and alkanediammonium ions are unable to approach effectively the exchange spots to displace the adsorbed diquat^{2+}. The exchange of diquat^{2+} with tetraalkylammonium ions from this mineral, contrasted sharply with the bentonite and vermioulite systems where the effectiveness of exchange was inversely related to ionic size. Moreover, the extent of desorption from Laponite by the tetraalkylammonium and by long chain surface active ions is much higher compared to the other two minerals. The results have been explained on the basis of its greater swelling characteristics due to lower charge density and consequently much smaller energy requirement for layer expansion for entry of large organic cations for exchange to occur.

Here also the plots of log (selectivity coefficient) against hydrated ionic radius and $1/a^{o}$ are linear with the alkaline earth metal ions while the latter plot

only is linear for the alkali metal ions.

The adsorption isotherm of the herbicide on Na-chlorite is as msual of H-type indicating strong affinity of the adsorbate for the adsorbent and the sorption data conform to the Langmuir equation. Infrared spectral analysis of the diquat-chlorite complex suggests the formation of charge-transfer complex as in bentonite and Laponite.

The desorption curves with inorganic ions are almost similar to those obtained earlier in the other minerals but the extent of release of diquat^{2+} from the chlorite matrix is much higher. This suggests that the herbicide cation is less strongly held by the mineral.

In this case also, the plots of log (selectivity coefficient) against hydrated ionic radius and $1/a^{o}$ of the alkaline earth metal ions are linear while for the alkali metal ions, the latter curve only shows linearity.

Steric hindrance as well as cation size in ion exchange with tetraalkylammonium ions is again demonstrated here as noted in bentonite and vermiculite, while the more freely expanding, lower layer charge Laponite did not exhibit this phenomenon. However, the exchange with long chain surface active ions and alkanediammonium ions increases with the size of the ions as observed in other minerals.

The exchange isotherms of diquat^{2+} onto Amberlite IR-120 (a strong cation exchange resin) and Amberlite IRC-50 (a weak cation exchange resin) also belong to the high affinity class in the classification of isotherms of Giles et al. The exchange data in both the resins obey the Langmuir equation. However the maximum exchanges of the herbicide cation onto Na-Amberlite IR-120 and Na-Amberlite IRC-50 are 390 me/100 gm and 540 me/100 gm respectively as against their c.e.c. values of 468 me/100 gm and 1030 me/100 gm. The lower exchange values may be caused by the physical inaccessibility of the resins to the large-sized diquat^{2+} ions.

The desorption isotherms of monovalent and bivalent inorganic ions are very similar to those obtained in clay minerals. On the basis of the extent of exchange as well as distribution and selectivity coefficients, the ions may be placed in the order: Li $<$ H $<$ Na $<$ NH_4 $<$ K $<$ Rb $<$ Cs and Mg $<$ Ca $<$ Sr $<$ Ba in Amberlite IR-120 while in Amberlite IRC-50 the sequence is NH_4 $<$ Li $<$ Na $<$ K $<$ Rb $<$ Cs and Mg $<$ Ca $<$ Sr $<$ Ba . The variable position of NH_4^+ and H^+ in the series is to be noted. The non-spherical nature of NH_4^+ may be responsible for its anomalous behaviour. The greater exchangeability of H^+ has been explained by assuming H^+ to be present as a bare proton in exchange reactions. The percentages of the release of

diquat^{2+} by the inorganic ions are found to be higher in Amberlite-IR-120 than in Amberlite IRC-50 suggesting that the herbicide cation is more strongly bound in the latter. Moreover, the extent of desorption with the inorganic ions is also higher than in the clay minerals studied except chlorite.

As in clay minerals, a sharp break is noted for both the resins in the plot of log (selectivity coefficient) vs hydrated ionic radius of the monovalent ions but against $1/a^{o}$, a good straight line is obtained. With the bivalent ions, however, both the parameters yield linear correlation.

To ascertain the role of ionic hydration in the exchange reactions, the desorption experiments with the inorganic ions have also been carried out in 50% ethanol-water (V/V) medium. It has been noted that the extent of desorption of diquat^{2+} from the resin matrices is higher than in the pure aqueous medium. The behaviour has been attributed to the altered solvation of these ions, the resulting ionic sizes, their activities and dielectric constant effects on coulombic interactions.

The extent of desorption of diquat^{2+} from both the resin matrices by the organic ions is found to be inversely related to ionic size or chain length except in Amberlite

IRC-50 with alkane diammonium ions at higher concentrations. The amount of desorption is also much smaller than with inorganic ions. The size of the organic ions may be too big to pass another ion into the narrow cavity of the rigid non-swelling resin framework and the results have been interpreted in terms of the steric factor, space requirement and difficulties of packing of these large organic cations in the resin structure. The exchange isotherms with $(CH_3)_4N^+$, $(C_2H_5)_4N^+$ and DTA^+ are S-shaped in both the resins indicative of cooperative sorption. However, compared to the other organic ions, a higher affinity for both the resins was observed with the alkane diammonium ions. Due to their short chain structure, possibly these ions experience less steric hindrance and also owing to their double charge sites in the structure, an important contribution of van der Waals interaction probably causes the higher affinity of the alkanediammonium ions for the resin surface.

The sorption isotherm of the herbicide on Na-molecular sieve-13X is of L-type and exchange data fit well in the linear form of the Langmuir equation. The maximum level of exchange is found to be only 18% of total o.e.c. of the molecular sieve-13X. This low exchange capacity may be caused due to physical unavailability of

different exchange sites to the big herbicide cations.

The DTA/DTG studies of clay-diquat and molecular sieve-diquat complexes show remarkable stability of the organic cation upto very high temperatures suggesting that under field conditions even in tropical countries, there is very little possibility of decomposition of the herbicide.

The order of desorption of diquat^{2+} from molecular sieve by monovalent inorganic ions at low concentrations is Li < Na < Cs < NH_4 < Rb < K while at higher concentrations the sequence is Li < Cs < Rb < Na < NH_4 < K. This type of sequence has not been observed in the present work with other adsorbents. The bivalent ions, however, follow the usual order: Mg < Ca < Sr < Ba.

As in other adsorbents, in this case also the plots of log (selectivity coefficient) vs hydrated ionic radius and $1/a^o$ are linear with the bivalent inorganic ions whereas for the monovalent ions the latter plot is only linear.

The extent of release of the herbicide from the molecular sieve by the tetraalkylammonium and long chain surfactants is found to be very meagre compared to the clay minerals and resins. This is probably due to the fact that because of its rigid three-dimensional framework

enclosing cavities, which are entered through windows of definite dimensions, exchange in molecular sieve-13X is greatly influenced by steric and space factors. With tetraalkylammonium and alkanediammonium ions the exchange is found to be inversely related to size of the ions while with the long chain surface active ions the reverse effect is observed. The exchange isotherm with $(CH_3)_4N^+$ is found to be S-shaped as noted in resins, suggesting that more and more exchange sites are accessible with the progress of exchange. The upper limits of exchange with alkanediammonium ions are found to be much higher than the other organic ions probably because these ions experience less steric hindrance due to their short chain structure.

It is clear from the above discussion that various attempts have been made to present a comprehensive picture on different aspects of exchange-equilibrium and the interaction of the bipyridylium herbicide, diquat, with clay minerals and other model adsorbents. In respect of sorption and desorption characteristics some uniformity has been observed while bentonite, vermiculite, Laponite, chlorite are the exchangers. With regard to the exchange characteristics, the carboxylated and sulphonated resins and the molecular sieve-13X exhibit a somewhat different character. This is however understood when the peculiarities

of the latter exchangers is recalled (pp160,166,191). The orders of preference of the inorganic and organic ions for the clay minerals, resins and the molecular sieve-13X against the herbicide cation are summarised below : (Cf. Table 17).

Table 17 speaks for itself. Although in point of this exchange-behaviour, the aluminosilicates are almost similar, occasional differences originate from their architectural dissimilarities as also from specificities of certain ions which are involved in the process. As pointed out earlier (P 84), the hydration energy of the ions plays a significant role in such a fixation process. This is also in agreement with the expected values of the distribution and selectivity coefficients.

The sequences of desorbing ions have been justified in terms of charge density and swelling properties of the adsorbents as well as of size, shape and steric hindrance of the adsorbate ions. It should also be mentioned, in the conclusion, that throughout the present investigation attempts have been made to explain the data in quantiative language whenever possible. For this purpose, valuable theoretical model (P 38) has been employed.

Table - 17

The order of preference of the ions for the silicate, resin and molecular sieve surface against diquat^{2+} cation.

Exchanger	Inorganic ions	Organic ions
H-bentonite-diquat complex	Li < Na < H < K < NH_4 < Rb < Cs	$(C_4H_9)_4N$ < $(C_3H_7)_4N$ < $(C_2H_5)_4N$ < $(CH_3)_4N$ < DTA < DDTA < CTA < CP
	Mg < Ca < Sr < Ba	EDA < PrDA < BuDA
Na-bentonite-diquat complex	Li < Na < H < NH_4 < K < Rb < Cs	$(C_4H_9)_4N$ < $(C_3H_7)_4N$ < $(C_2H_5)_4N$ < $(CH_3)_4N$ < DTA < DDTA < CTA < CP
	Mg < Ca < Sr < Ba	EDA < PrDA < BuDA
Na-vermiculite-diquat complex	Li < H < Na < K < NH_4 < Rb < Cs	$(C_4H_9)_4N$ < $(C_3H_7)_4N$ < $(C_2H_5)_4N$ < $(CH_3)_4N$ < DTA << DDTA < CTA < CP
	Mg < Ca < Sr < Ba	EDA < PrDA < BuDA

Contd..

Table - 17 (Contd..)

Exchanger	Inorganic ions	Organic ions
Na-Laponite-diquat-complex	Na < K < Li < NH_4 < Rb < Cs < H	$(CH_3)_4N$ < $(C_2H_5)_4N$ < $(C_3H_7)_4N$ < $(C_4H_9)_4N$ << DTA < DDTA < CTA << CP
	Mg < Ca < Sr < Ba	EDA < PrDA < BuDA
Na-chlorite-diquat-complex	Li < Na < H < K < NH_4 < Rb < Cs	$(C_4H_9)_4N$ << $(C_3H_7)_4N$ << $(C_2H_5)_4N$ << $(CH_3)_4N$ << DTA << DDTA < CTA < CP
	Mg < Ca < Sr < Ba	EDA < PrDA < BuDA
Na-IR-120-resin-diquat complex	Li < H < Na < NH_4 < K < Rb < Cs	$(C_4H_9)_4N$ < CP < CTA < $(C_3H_7)_4N$ < DDTA < $(C_2H_5)_4N$ < DTA < $(CH_3)_4N$
	Mg < Ca < Sr < Ba	BuDA < PrDA < EDA

Contd..

Table - 17 (Contd..)

Exchanger	Inorganic ions	Organic ions
Na-IRC-50 resin-diquat complex	Li < Na < K < Rb < Cs < NH_4 ≤ H at low concentrations and NH_4 < Li < Na < K < Rb < Cs < H at higher concentrations.	$(C_4H_9)_4N$ < $(C_3H_7)_4N$ < $(C_2H_5)_4N$ < $(CH_3)_4N$ < CTA < CP ≤ DTA
	Mg < Ca ≤ Sr < Ba	BuDA < PrDA < EDA at low concentrations and EDA < PrDA < BuDA at higher concentrations
Na-molecular sieve-X-diquat complex	Li < Na < Cs < Rb < NH_4 < K at low concentrations and Li < Cs < Rb ≤ Na < NH_4 < K at higher concentrations	$(C_4H_9)_4N$ < $(C_3H_7)_4N$ < $(C_2H_5)_4N$ < $(CH_3)_4N$ < DTA < DDTA < CTA < CP
	Mg << Ca << Sr < Ba	BuDA << PrDA < EDA

In addition to different quantitative methods, empirical approaches have also been given their due credit for a satisfactory interpretation of the experimental data.